

Oxide-cluster nucleation, growth, and saturation on Si(001)-(2×1) surfaces: Atomic-scale measurements and models

J. V. Seiple, C. Ebner, and J. P. Pelz

Department of Physics, The Ohio State University, Columbus, Ohio 43210

(Received 4 October 1995; revised manuscript received 20 February 1996)

Nucleation rates for oxide clusters on Si(001)-(2×1) surfaces have been determined as functions of temperature (600–650 °C), pressure (2×10^{-8} – 1.2×10^{-7} torr), and dose (≤ 1200 L) by counting oxygen related pinning sites in scanning tunneling microscopy images. The low-dose temperature dependence indicates that the nucleation mechanism is related to thermally activated processes. At high doses, the nucleation rate was suppressed, while the vertical etch rate remained constant. Simulations of these high-dose experiments indicate good agreement with a dual-species oxidation model, but not with a single-species model. [S0163-1829(96)01923-6]

The nucleation and growth of oxide films on Si surfaces at elevated temperatures is of critical importance for a variety of applications, ranging from the controlled growth of ultrathin, high-quality oxide films used as gate dielectric materials in field-effect transistor devices, to the prediction and control of surface roughening during transient exposure to residual oxygen and/or water vapor in modern integrated processing chambers.^{1,2} However, despite extensive study of the initial oxidation of silicon,^{2–15} the fundamental atomic-scale mechanisms underlying submonolayer oxide nucleation and growth are still not well established. A number of atomic-scale models have been proposed and compared with *macroscopic* measurements of Si surface oxidation over a range of temperatures and oxidation pressures,^{5,6,10,11} but to date little³ has been done to directly compare *microscopic* predictions of these models with microscopic measurements of oxide nucleation and growth kinetics. Such a direct comparison would be an important test of the validity of competing atomic-scale models.

We have used an ultrahigh vacuum scanning tunneling microscope (UHV STM) to examine submonolayer oxide-cluster nucleation on Si(001) surfaces after oxidation at sample temperatures, T_s , in the range 600–650 °C, oxygen pressures, P_{ox} , in the range 2×10^{-8} – 1.2×10^{-7} torr, and O_2 exposures, D_{ox} , as high as 1200 L, where $1 \text{ L} \equiv 10^{-6}$ torr s. Under these conditions oxidation-induced surface etching is the dominant process, but oxide-cluster nucleation also occurs and produces “pinning sites,” which can be directly counted.^{2–4,14} We find that (1) the initial oxide-cluster nucleation rate is temperature dependent, consistent with a nucleation mechanism that is related to thermally activated processes; (2) oxide nucleation is strongly suppressed at high O_2 doses ($D_{ox} > \sim 200$ L), even though the O_2 coverage remains much less than one monolayer; and (3) the vertical surface etch rate η at locations *between* nucleation sites remains roughly constant. Taken together, these observations impose rather restrictive constraints on possible atomistic models. We have used rate equation analysis and Monte Carlo simulations to check different models, and find that a “single-oxide-species” diffusional model is insufficient to account for *both* suppressed nucleation and constant etching,

while a dual-species diffusional model (such as that proposed by Engstrom *et al.*⁵) is consistent with the observed data. This provides the first direct *atomic-scale* support for such a dual-species model.

All scans were measured at room temperature following oxygen exposure at elevated temperatures. Two oxidation procedures were used. For procedure “A,” Si(001) samples (*n*-type, 0.05 Ω cm, miscut 0.25° toward [110]) were (1) resistively “flashed” at 1250 °C, (2) quenched to room temperature, (3) characterized with STM, (4) heated to temperature and exposed to O_2 , and (5) quenched to room temperature and scanned. For some experiments, a temperature gradient was established across the sample¹⁰ during oxidation and the temperature-vs-position profile was measured with an infrared pyrometer. We could then scan different areas of the sample to directly monitor the temperature dependence of the oxide nucleation. For procedure “B,” a “pre-etch” was used to further clean the surface. Samples were (1) flashed at 1250 °C, (2) pre-etched by cooling to 900 °C and exposing to 6×10^{-8} torr of O_2 for 14 min, (3) cooled further to the oxidation temperature (600–650 °C) and exposed to O_2 (at 3×10^{-8} – 1.2×10^{-7} torr), and (4) quenched to room temperature and scanned. The temperature-pressure conditions during step (2) produce *only* surface etching,^{2,10} which removes the top two to three Si layers. Occasionally, samples would be quenched directly following the 900 °C etch and scanned, verifying that this step does *not* itself nucleate oxide clusters. Both oxidation procedures yielded cluster densities within a factor of 2 from each other, with the pre-etch procedure (used to measure dose dependence) resulting in slightly fewer pinning sites.

We have previously shown that characteristic defects occur after oxidation at elevated temperatures, and argued (based on strong P_{ox} dependence and annealing behavior) that these defects are in fact small oxidized regions.^{2,3} We find that these oxidized sites evolve into complex disordered regions at higher doses, pin step edges during surface etching, and eventually develop into isolated island structures. Here, we refer to these structures as simply “oxide clusters.”

We first address the temperature dependence of the initial oxide-cluster nucleation rate J_{ox} . Figures 1(a) and 1(b) show

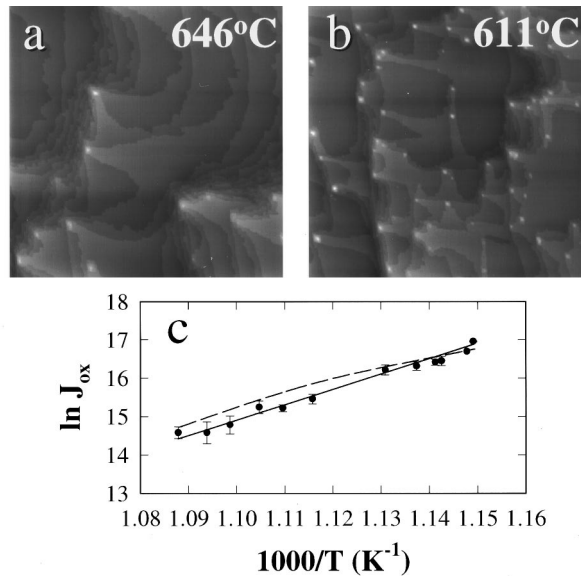


FIG. 1. Oxide-cluster nucleation on a Si(001) sample with a $\sim 50^\circ\text{C}$ temperature gradient exposed to 150 L O_2 at 6×10^{-8} torr. (a) STM top-view gray scale image of “hot” part of sample ($T_s \approx 646^\circ\text{C}$). (b) Image of “cold” part ($T_s \approx 611^\circ\text{C}$), showing more oxide clusters than the hot part. (c) Dependence of J_{ox} on inverse temperature for entire sample. The best-fit line (solid) indicates an effective activation energy $E_{\text{eff}} \approx -3.5$ eV (see text). The dashed line is the dual-species model prediction. J_{ox} is in units of $\text{cm}^{-2} \text{s}^{-1}$.

top-view gray scale images of two different $0.5 \times 0.5 \mu\text{m}^2$ areas of a sample, which had a $\sim 50^\circ\text{C}$ temperature gradient across it during oxidation at $P_{\text{ox}} \approx 6 \times 10^{-8}$ torr and $D_{\text{ox}} \approx 150$ L. Since these measurements were both made following a *single* oxidation, they permit us to directly monitor the temperature dependence of J_{ox} with all other experimental variables (e.g., P_{ox} , D_{ox} , initial surface defect density, etc.) held fixed. The number of oxide clusters (visible as small raised bumps at the ends of pinned step fingers^{2,3}) is clearly greater at the low-temperature side of the sample.

Figure 1(c) shows a semilog plot of J_{ox} versus inverse temperature determined by counting oxide clusters at different temperature positions across the sample and dividing by the oxidation time. The solid curve shows the best-fit straight line, with a slope consistent with an *effective* activation energy $E_{\text{eff}} \approx -3.5$ eV. As we discuss below, this temperature dependence is not due to a *single* thermally activated process with a negative energy (which is unphysical), but rather results from a *combination* of activated processes (including desorption, nucleation, diffusion, etc.).^{3,4} Many such experiments have been done at doses ranging from 50 to 200 L over a similar temperature range, and in all cases the resulting data were approximately linear on such a semilog plot, with $-4.0 < E_{\text{eff}} < -3.3$ eV.² The dashed curve shows the prediction of the dual-species model, which will be discussed later.

We next address the dose dependence of the oxide-cluster nucleation. Figures 2(a) and 2(b) show $0.3 \times 0.3 \mu\text{m}^2$ scans of two oxidations done at the same temperature (600°C) and O_2 pressure (6×10^{-8} torr), but for a total O_2 dose of 400 and 800 L, respectively.² The data sets are shown as top-view gray scales, as well as three-dimensional (3D) perspec-

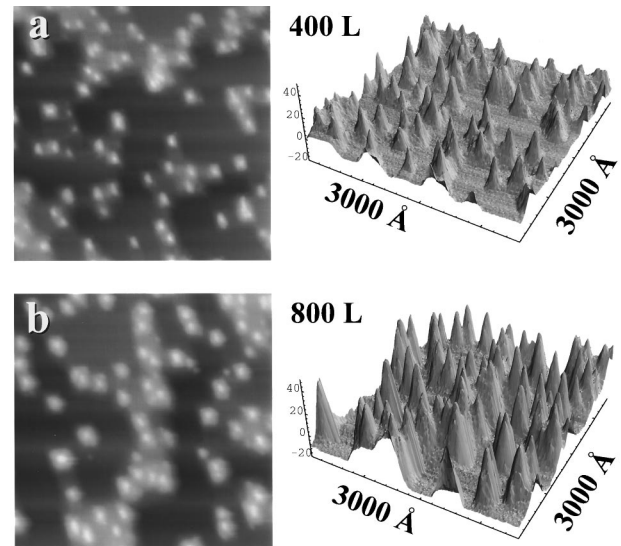


FIG. 2. Top-view gray scale and 3D perspective views of Si(001) surface after oxidation at 600°C , 6×10^{-8} torr, and doses of (a) 400 L and (b) 800 L. Both doses result in approximately the same number density of oxide clusters (indicating that new cluster nucleation has been suppressed), while the clusters are roughly twice as high at the larger dose (indicating a roughly constant vertical etch rate between clusters).

tives to make two specific points. The first point, seen most clearly from the top view, is that doubling the exposures still results in approximately the same number of clusters on the surface [77 each in Figs. 2(a) and 2(b)]. *This indicates that, at high doses, the oxide-cluster density saturates.* The second point, evident from the perspective view, is that the *height* of the clusters at 800 L has increased to roughly twice the height at 400 L. We find that the height increases almost linearly with dose,² indicating that the vertical etch rate η remains roughly constant on the clean terrace areas between the clusters. Close-up scans of the areas *between* the islands (not shown) indicates that the 2×1 dimer reconstruction is still intact and is *not* covered with an oxide layer.

This saturation behavior was examined as a function of temperature and pressure. Figure 3 shows the number density of oxide clusters as a function of layers etched for discrete temperatures at a constant pressure of $\sim 6 \times 10^{-8}$ torr [Fig. 3(a)] and for discrete pressures at a constant temperature of 650°C [Fig. 3(b)]. Note that an O_2 dose of 25 L etches approximately one layer of silicon.^{2,3} In general the cluster density increases with dose up to ~ 5 layers etched, at which point it saturates at a level, which increases with lower temperature and higher pressure. The data points were measured experimentally, and the fits are explained below.

Previously, we considered a simple model for oxide-cluster nucleation,^{3,4} which assumed that reacted-oxygen dissociates on the surface to form diffusing “oxide monomers.” These could either etch the surface (via the desorption of SiO), join with another monomer to nucleate an oxide cluster, or attach to an existing cluster. Rate equation analysis and Monte Carlo simulations were used to examine the evolution of oxide clusters in time as a function of P_{ox} and T_s .⁴ At low doses (< 100 L), predictions of this simple single-species model were consistent with the mea-

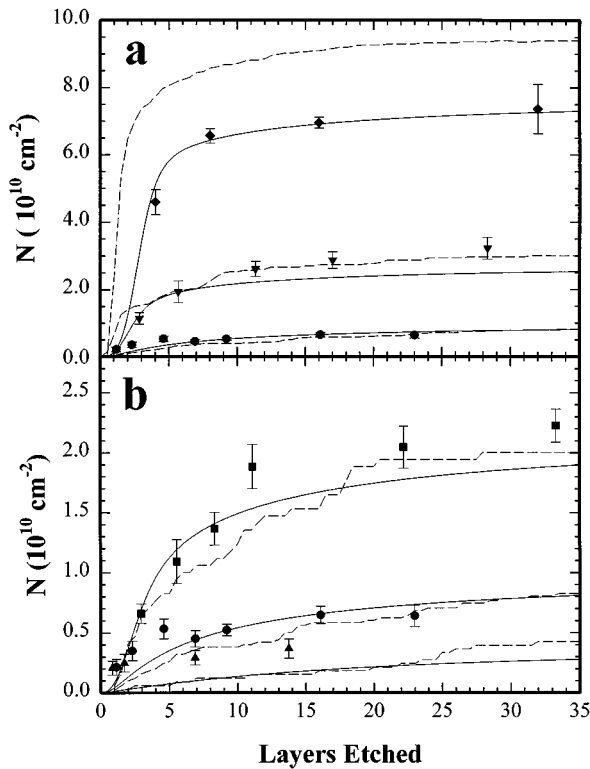


FIG. 3. Oxide-cluster saturation curves as a function of layers etched. Dashed lines are generated from Monte Carlo simulations and solid lines from integrated rate equations, both using the two-species model described in the text. In (a), oxidations were done at a constant pressure of 6×10^{-8} torr and 600, 625, and 650 °C (top to bottom). In (b), oxidations were done at a constant temperature of 650 °C and 12, 6, and 3×10^{-8} torr (top to bottom).

sured pressure dependence³ and temperature dependence (Fig. 1 and Ref. 3) of the initial nucleation rate J_{ox} , assuming reasonable values for parameters controlling SiO desorption, monomer diffusion, and cluster nucleation.

However, we find that this single-species model cannot account for the observed high-dose suppression of J_{ox} together with the observed constant vertical etch rate.⁴ In the single-species model^{3,4} $J_{\text{ox}} \sim Dn_1^2 \exp(-\beta E_n)$, where n_1 is the density of diffusing monomers, E_n is an activation barrier for two monomers to “nucleate” a cluster, and D is the surface diffusion coefficient for the monomers. According to conventional nucleation models,¹⁶ growing clusters suppress nucleation of new clusters by acting as efficient sinks for the diffusing monomers. This reduces n_1 , which in turn suppresses J_{ox} . In the single-species model, however, desorption of the diffusing monomers also produces surface etching,^{3,4} with the etch rate η dependent on n_1 as $\eta \sim n_1/\tau$, where τ the desorption lifetime for monomers. Hence the nucleation rate J_{ox} and the etch rate η should be directly linked, since a reduction in n_1 should suppress both J_{ox} and η . Experimentally, however, we measure a strong suppression in J_{ox} , but no measurable change in η . Several extensions to the single-species model were considered (e.g., cluster coalescence and “two-cluster” break up⁴), but still we could not find a set of conditions that suppressed nucleation without also suppressing etching.

We now consider a different model, which lessens the

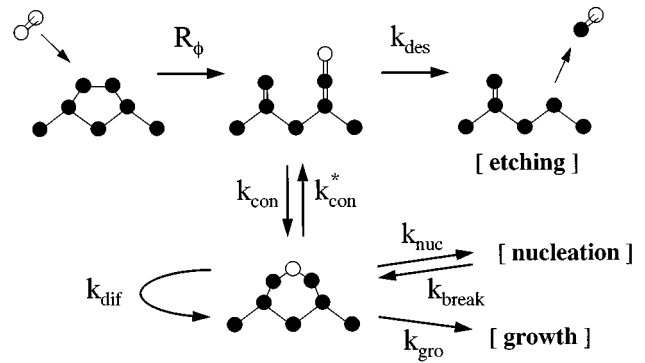


FIG. 4. Schematic of a two-species oxidation model, adapted from Ref. 5. Oxygen (silicon) atoms shown as empty (filled) circles. See text for parameter values.

interdependence of J_{ox} and η by assuming that two *different* oxide-monomer species are responsible for SiO desorption and oxide-cluster nucleation, respectively. In fact, such a model has already been proposed by Engstrom *et al.*,⁵ based entirely on macroscopic measurements of oxide growth and SiO desorption. This model (shown schematically in Fig. 4) assumes that reacted-oxygen atoms first dissociate to form a “desorption precursor” configuration (top-center Fig. 4), which can either desorb from the surface as SiO (at rate k_{des}), or convert (at rate k_{con}) to a bridge- or back-bonded configuration (bottom-center Fig. 4), which in turn can diffuse across the surface (at rate k_{dif}) and lead to oxide-cluster nucleation (at rate k_{nuc}) or growth (at rate k_{gro}). Clusters of two were allowed to break up (at rate k_{break}), while clusters of three or more were assumed stable.⁴ A necessary requirement for this type of model to account for the observed behavior is that $k_{\text{des}} \gg k_{\text{con}}$. In this case, η remains roughly constant since most reacted-oxygen atoms simply desorb as SiO before they convert to the back-bonded form. However, the population of the (minority) back-bonded species that does form shows large variations with time, and becomes depleted when a sufficient oxide-cluster density develops. Hence, cluster nucleation is suppressed at higher doses without significantly affecting η .

Rate equation modeling (solid lines in Fig. 3) was done for this system and a qualitative consistency could be obtained with the measured data using reasonable values for the various parameters. The model’s predictions show the correct temperature and pressure dependencies for the saturation cluster density, and the saturation onset at approximately five layers etched. Monte Carlo simulations (dashed lines in Fig. 3) with similar parameter values also show the correct qualitative behavior. Simulations of this dual-species model are also reasonably consistent with the *initial* nucleation rate J_{ox} measured for doses ≤ 150 L, as shown by the dashed curve in Fig. 1(c). These simulations also do result in a nearly constant vertical etch rate η over the duration of the simulations (not shown).

Since most reacted-oxygen atoms desorb as SiO, the reacted-oxygen flux rate R_ϕ [equal to the incident oxygen flux times a sticking coefficient of about 4% (Ref. 2)] could be estimated directly from the measured etch rate for each curve.² The activation energy ($E_{\text{des}} = 3.3$ eV) and prefactor ($4 \times 10^{18} \text{ s}^{-1}$) for k_{des} were taken from Ref. 5. The other activation energies in the rate equation analysis were

$E_{\text{con}} = E_{\text{con}}^* = 2.8$ eV, $E_{\text{dif}} + E_{\text{nuc}} = 2.6$ eV, $E_{\text{dif}} + E_{\text{gro}} = 2.2$ eV, and $E_{\text{break}} = 2.25$ eV. For simplicity, all prefactors (except for k_{des}) were set equal to $5.0 \times 10^{12} \text{ s}^{-1}$. Note that the rate for cluster nucleation is assumed equal to the *product* of a monomer diffusion term times a reaction probability $P_{\text{nuc}} = \exp(-E_{\text{nuc}}/k_B T)$ (with analogous terms for cluster growth), so that only the *sum* energies $E_{\text{dif}} + E_{\text{nuc}}$ and $E_{\text{dif}} + E_{\text{gro}}$ appear in the rate equations. Here, E_{nuc} and E_{gro} would presumably correspond to a bond-breaking energy required to form a cluster. The capture number for a stable cluster was proportional to the cluster perimeter. We should also note that the ‘‘precursor’’ species may diffuse as well, but since it does not directly lead to nucleation or growth, its diffusion rate has no bearing on the model predictions.

Admittedly, this model contains a number of adjustable parameters, which are not known accurately from independent measurements. However, the values do appear reasonable. We expect that the surface oxygen diffusion energy E_{dif} should be less than the *bulk* diffusion energy of 2.4 eV (Ref. 17), so the energy sums $E_{\text{dif}} + E_{\text{nuc}} = 2.5$ eV and $E_{\text{dif}} + E_{\text{gro}} = 2.1$ eV can easily be satisfied with moderate, nonzero values for E_{nuc} and E_{gro} . In fact, these values are roughly consistent with reported values for surface oxygen diffusion $E_{\text{dif}} = 1.0$ eV (Ref. 18), and oxide growth $E_{\text{gro}} = 1.6$ eV (Ref. 11). The main point here is that this dual-

species model with a single set of reasonable parameter values shows very good qualitative consistency, with the pressure and temperature dependencies of initial oxide-cluster nucleation, growth, and saturation. This lends strong *microscopic* support for a dual-species oxidation model such as that proposed by Engstrom *et al.*⁵

Finally, we note that these STM measurements can give direct information about typical diffusion lengths for surface oxygen. In order for existing clusters to suppress the nucleation of new clusters, the surface diffusion length L_{dif} must be at least as long as the typical cluster spacing L_{clus} . For example, we see from Fig. 3(b) that at saturation $L_{\text{clus}} > 100$ nm at 650°C and $P_{\text{ox}} = 6 \times 10^{-8}$ torr, which sets a lower limit of ~ 100 nm for the L_{dif} under these conditions. This limit is well within the simulated diffusion lengths with the parameter values assumed above.

In summary, we have observed temperature-dependent oxide nucleation on Si(001)-(2 \times 1) surfaces, with distinct oxide-cluster saturation at high doses, and with a nearly constant vertical etch rate between clusters. These data are inconsistent with a simple single-species diffusional model, but show good qualitative agreement with a dual-species diffusional model.⁵

This work was supported by NSF Grant Nos. DMR-9357535 and DMR-9406936, and PRF Grant No. 26647-G5.

¹M. Offenberger, M. Liehr, and G. W. Rubloff, *J. Vac. Sci. Technol. A* **9**, 1058 (1991).

²J. V. Seiple and J. P. Pelz, *J. Vac. Sci. Technol. A* **13**, 772 (1995).

³J. V. Seiple and J. P. Pelz, *Phys. Rev. Lett.* **73**, 999 (1994).

⁴C. Ebner, J. V. Seiple, and J. P. Pelz, *Phys. Rev. B* **52**, 16 651 (1995).

⁵J. R. Engstrom, D. J. Bonser, M. M. Nelson, and T. Engel, *Surf. Sci.* **256**, 317 (1991).

⁶M. P. D’evelyn, M. M. Nelson, and T. Engel, *Surf. Sci.* **186**, 75 (1987).

⁷M. L. Yu and B. N. Eldridge, *Phys. Rev. Lett.* **58**, 1691 (1987).

⁸K. Wurn *et al.*, *Phys. Rev. B* **50**, 1567 (1994).

⁹M. Udagawa, M. Niwa, and I. Sumita, *Jpn. J. Appl. Phys.* **33**, 375 (1994).

¹⁰F. W. Smith and G. Ghidini, *J. Electrochem. Soc.* **129**, 1300 (1982).

¹¹V. D. Borman, E. P. Gusev, Yu. Yu. Lebedinski, and V. I. Troyan, *Phys. Rev. B* **49**, 5415 (1994).

¹²F. M. Ross, J. M. Gibson, and R. D. Twisten, *Surf. Sci.* **310**, 243 (1994).

¹³A. Feltz, U. Memmert, and R. J. Behm, *Surf. Sci.* **314**, 34 (1994).

¹⁴F. Donig *et al.*, *J. Vac. Sci. Technol. B* **11**, 1955 (1993).

¹⁵J. Seiple, J. Pecquet, Z. Meng, and J. P. Pelz, *J. Vac. Sci. Technol. A* **11**, 1649 (1993).

¹⁶H. Brune, H. Röder, C. Boragno, and K. Kern, *Phys. Rev. Lett.* **73**, 1955 (1994).

¹⁷J. C. Mikkelsen, *Appl. Phys. Lett.* **40**, 336 (1982).

¹⁸M. Lozano and M. Tringides, *Europhys. Lett.* **30**, 537 (1995).